Изв.Крымской Астрофиз.Обс. 101, 51–57 (2005)

ИЗВЕСТИЯ
КРЫМСКОЙ
АСТРОФИЗИЧЕСКОЙ
ОБСЕРВАТОРИИ

УДК 524.7

Two-Wavelength Observations of BL Lac Object in 2002

V.V. Fidelis

Crimean Astrophysical Observatory, 98409, Ukraine, Crimea, Nauchny

Поступила в редакцию 20 мая 2004 г.

Аннотация. Двухволновые наблюдения объекта BL Lac в 2002 году.

В 2002 году были проведены квази-одновременные двухволновые наблюдения прототипа галактик с нестационарными ядрами – объекта BL Lac в диапазоне сверхвысоких энергий (СВЭ) с помощью наземного телескопа ГТ-48 и в рентгеновском диапазоне по данным регистрации детектором ASM на борту рентгеновской обсерватории RXTE. Наблюдения продолжались с 7 июля по 2 декабря 2002 г. Результаты экспозиции источника в течении 8 часов и 10 минут показали избыток гамма-квантов СВЭ в направлении наблюдавшегося объекта со статистической достоверностью 5.6 σ. Оценка интегрального потока от BL Lac дала величину, равную (1.1 ± 0.4) Crab (E $\geq$ 1 TeV).

В целом, как в диапазоне СВЭ, так и в рентгеновском диапазоне, наблюдалась тенденция повышение активности объекта к концу наблюдений, а средние значения потоков в различные безлунные периоды коррелировали с коэффициентом корреляции, равным ≈0.65.

Two-Wavelength Observations of BL Lac Object in 2002, *by V.V. Fidelis.* Quasi-simultaneous two-wavelength observations of BL Lac object, the prototype of galaxies with variable nuclei, were taken at Very High Energy (VHE) band with the aid of ground-based telescope GT-48 and in X-rays from ASM/RXTE observations in 2002. The time coverage continued from July to December 2002.

The results of source exposure during 8 hrs and 10 min have shown the excess of VHE gamma-quanta in the direction of observed object at the 5.6 σ confidence level. The estimation of the integral flux from BL Lac has given the value, equal to (1.1 ± 0.4) Crab (E $\geq$ 1 TeV).

In a whole in VHE band as well in X-rays was observed enhanced activity to the end of observations and average fluxes in different moonless periods were correlated with the correlation coefficient equal to ≈0.65.

Keywords: gamma rays: observations – galaxies: BL Lacertae objects: individual: BL Lac

1 Introduction

Detection of high-energy γ-ray emission from a number of Active Galactic Nuclei (AGNs) by the ECRET detector onboard the Compton Gamma-ray Observatory (Thompson et al., 1995) has stimulated the search for γ-ray emission from them in VHE band. This emission may be registered only with using sophisticated technique based on the air Cerenkov detectors.

The principle of Cerenkov technique is provided by nature: due to interaction with atmospheric nuclei VHE γ-quanta may be registered through natural effect – Cerenkov light emission. Entering into Earth's atmosphere VHE photons give their energy to electromagnetic Extensive Air Showers (EAS). Some fast-moving particles in these showers generate visible Cerenkov light flashes that may be detected on the ground (Bonnet-Bidaud and Chardin, 1988). Observation of EAS by two or more Cerenkov telescopes spaced apart by distance not more than the radius of Cerenkov light pool allows effectively reconstruct the arrival direction of individual γ-ray showers (Aharonian and Konopelko, 1997). A reported detection of VHE photons from the direction of extra-galactic objects is related only to the BL Lac class of AGNs, i.e. the objects having jets oriented close to the observer's line of sight (Punch et al., 1992; Quinn et al., 1996; Catanese et al., 1998; Aharonian et al., 2002, 2003b; Neshpor et al., 1998, 2001).

In BL Lac type objects TeV photons are commonly believed to originate in the relativistic jets, most popularly due to inverse Compton (IC) scattering of relativistic electrons on seed photons (Aharonian et al., 2003a). The most striking feature of the BL Lacs is their strong variability from the optical wavelengths to the VHE γ-rays. Temporal scales of their variability range in TeV band from tens of minutes (Aharonian et al., 1999) to years (Katarzynski et al., 1999).

It is well known that the higher energy of observed photons the lower flux from observed objects. So that investigation of AGNs needs continuous observations for accumulation statistics on different time scales.

The spectral energy distribution of BL Lacs is characterized by two broad peaks which may be referred to as synchrotron and IC components of emission (Ghisellini et al., 1998.). A tight correlation in the X-ray and TeV bands in some BL Lac objects can be accounted for one-zone homogeneous Synchrotron Self-Compton (SSC) model (Costamante and Ghisellini, 2002).

BL Lac was observed in TeV energy band in Whipple observatory in 1995. Only upper limit estimated as $\approx$0.06 Crab (E $>$ 350 GeV) was derived from Whipple observations (Catanese et al., 1997). At CrAO this object was detected in 1998 at the 7.2σ level with flux estimation equal to $(2.1 \pm 0.4)\cdot 10^{-11}ph\cdot$cm^{-2}s^{-1} (Neshpor et al., 2001).

BL Lac was the target of an extensive multi-wavelength monitoring campaign in radio band, optical frequencies, in X-rays (BeppoSAX and RXTE) and in VHE γ-rays (HEGRA) (Böttcher et al., 2003) in 2003. The observations had provided evidence that the synchrotron spectrum of the object extends out to $\sim$10 keV. So the simultaneous observations in X-ray and TeV band may allow us to investigate the variability of BL Lac and hence to determine the nature of the dominant radiation processes.

Correlation of TeV emission from BL Lac in 2002 with luminosity in optical band was investigated by Neshpor et al. (2003, 2004). In this work is studied correlation of TeV emission from this object in 2002 with X-rays.

2 The Cerenkov Telescope and Observations

Two observations of BL Lac object reported here were carried out in 2002 with air–Cerenkov telescope GT-48 and All Sky Monitor (ASM) onboard the Rossi X-ray Timing Explorer (RXTE) Project launched 1995. The ASM observes the brightest known X-ray sources for variability and also alert the community when new sources appear.

The GT-48 telescope at present consists of two identical alt-azimuth mountings (sections), Nortn (N) and South (S), separated apart by 20 m. Each section is equipped with four cameras consisting of 37 photomultiplier tubes (PMTs) that organize 37 channels. Each camera, mounted in the focal plane of four mirrors with diameters of 1.2 m, records the images of atmospheric Cerenkov radiation from air showers produced by γ-rays and cosmic rays (CR). Each PMT in camera is viewing a circular field of $0^{\circ}\!.2$ radius, a total field of view of each camera is $2^{\circ}\!.6$. Images of Cerenkov flashes are detected in the optical band (300 – 560 nm). The total area of mirrors are 36 m^2. The signals from the PMTs of four cameras on each section are linearly added.

Telescope operates in coincidence mode between two sections with time resolution of 15 ns. Flashes are registered only when the amplitudes of the signals for any two of the 37 channels are coincide in time and exceed the certain threshold. Both mountings are geared with the aid of control system with a pointing accuracy of $\pm 0^{\circ}\!.05$. The result of registration of flashes is a digitized forms of their images.

The threshold energy for detection of γ-rays was determined by numerical simulations and equals about 1 TeV (Kalekin, 1999). A detailed description of this apparatus can be found in Vladimirsky et al. (1994).

Observations of BL Lac were made in the ON/OFF mode, when ON runs duration by 35 minutes were followed by OFF runs with the same duration of background exposure. In ON runs the source was in the centre of the field of camera; in OFF runs the observing sky region was shifted on right ascension by 40 min. The pointing direction was ($\alpha = 22^h02^m48^s$ and $\delta = 42°17'15''$). The collected data were cleaned for weather conditions. This selecting criteria resulted in effective exposure time of 8 hours and 10 minutes, splitted between July and December 2002 observing periods (Table 1).

Table 1. BL Lac observation Log

Period	Dates	MJD	Source exposure (min)
I	July 7–15	52463 – 52471	175
II	September 4	52522	70
III	October 8–12	52556 – 52560	140
VI	November 2	52581	35
V	November 28– December 2	52607 – 52611	70
	Total	52463 – 52611	490

The cleaned data were followed by the next reduction process. 1) Events which were registered in the distorted telescope guiding process (i.e. deviation of the optical axis of the telescope from the specific direction exceeded $3'$) were disregarded. 2) Data in which was exceeded an analog–digital converter maximum (255 discrete units, or 180 photoelectrons) in at least one channel were thrown out. 3) Flashes whose maximum amplitude was in the outer ring of camera were disregarded. 4) Amplitudes of signals in all channels were corrected using calibration coefficients estimated in each run.

3 Image Analysis, Gamma/Hadron Separation

EAS may be induced not only by VHE γ-rays but also the cosmic rays (CR). Both types of showers may be separated by difference of their images and arrival directions. EAS from γ-ray primaries have compact forms of their images, small angular sizes and are oriented in the field of view to the source position. EAS from the CR, mainly protons, have more fragmented forms, higher angular dimensions and have arrived from all directions. Digitized flash images were processed using formal mathematical methods. First and second moments of the brightness distribution were calculated and from them were derived the coordinates of the centres of the brightness distribution, the effective *length* and effective *width* of each flash image (Figure 1).

The orientation of the image relative to the position of the γ-ray source in the focal plane of the camera is described by several parameters. They are: *alpha* – angle between the direction toward the source from the flash centre and the direction of the major axis of the flash image; *miss* – the perpendicular distance of the centre of the field (the source) from the image axis; *azwidth* – the r.m.s. image width relative to a new axis which joins the source to the centre of the image. Parameter *dist* describes the distance of image centre from source position in the field of view of camera (Hillas, 1985). Because three orientation parameters are connected with each other geometrically (Figure 1) only one of them jointly with parameter *dist* is used for processing of the Cerenkov light images.

Gamma-ray events were also selected by minimal amplitude of signal V because the parameters of flashes with low energy are derived with high errors. For distinguishing two types of flashes by forms of their images we have used imaging pattern ratio (IPR). It was assigned zero for the most compact images and 1 – 7 for more fragmented ones (0- simple flash, 1- no single array flash, 2- curve flash, 4- camel flash and others are their combination). Parameter IPR may be assigned individually for each section of telescope for the purpose of realization of maximal signal/noise ratio.

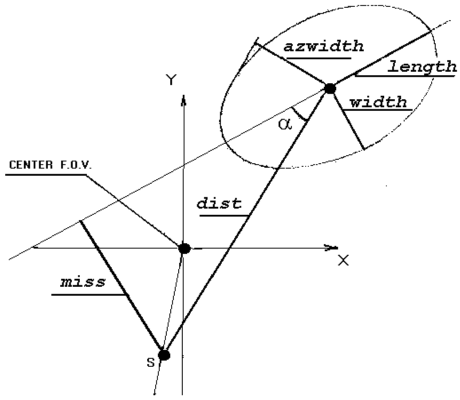

Fig. 1. Schematic representation of the parameters of Cerenkov flash image. O – the centre of brightness distribution, S – source position. Segment OS corresponds to angular parameter *dist*

The boundary values of parameters were selected in such a way, in order to the effect, described by expression $Q = (Ns - Nb)/\sqrt{Ns + Nb}$, i.e., the signal to noise ratio, is highest possible. Here Ns and Nb are the numbers of selected gamma-ray events detected during the observation in the direction of the source and background respectively. $N_\gamma = (Ns - Nb)$ is interpreted as a number of gamma-quanta and $\sqrt{Ns + Nb}$ as a error of this number. Events, having value of parameter, did not fall in the given interval, disregarded from consideration.

The images were processed with the software package and the following criteria for selection of showers, produced by gamma-quanta from a background of showers produced by CR are used:

1) $0.^\circ16 <$ *length* (N) $< 0.^\circ32$; $0.^\circ17 <$ *length* (S) $< 0.^\circ32$
2) $0.^\circ05 <$ *width* (N) $< 0.^\circ16$; $0.^\circ05 <$ *width* (S) $< 0.^\circ17$
3) $0.^\circ25 <$ *dist* (N) $< 0.^\circ95$; $0.^\circ05 <$ *dist* (S) $< 0.^\circ9$
4) 100<V(N)<300, 125<V(S)<450
5) IPR (N)=0; IPR(S)=0

Here N belongs to North section, S – Southern.

4 The Results of Analysis

After applying to ON/OFF data set cut we have obtained the following statistics (Table 2). Filtering cut includes selection by V, IPR, *length* and *width*. Selection by parameter *azwidth* was accomplished jointly with the parameter *dist*.

Table 2. Results of BL Lac observing data analysis

Period	Selection method	Ns	Nb	Ns – Nb	Q, σ
	Raw data	5941	5977	-36	-0.33
	Filtering	92	37	55	4.84
	$0.^\circ13<$*azwidth*$< 0.^\circ24$				
I		20	10	10	1.83
II		14	7	7	1.53
III		23	2	21	4.20
IV		8	2	6	1.90
V		15	2	13	3.15
Total		80	23	57	5.62

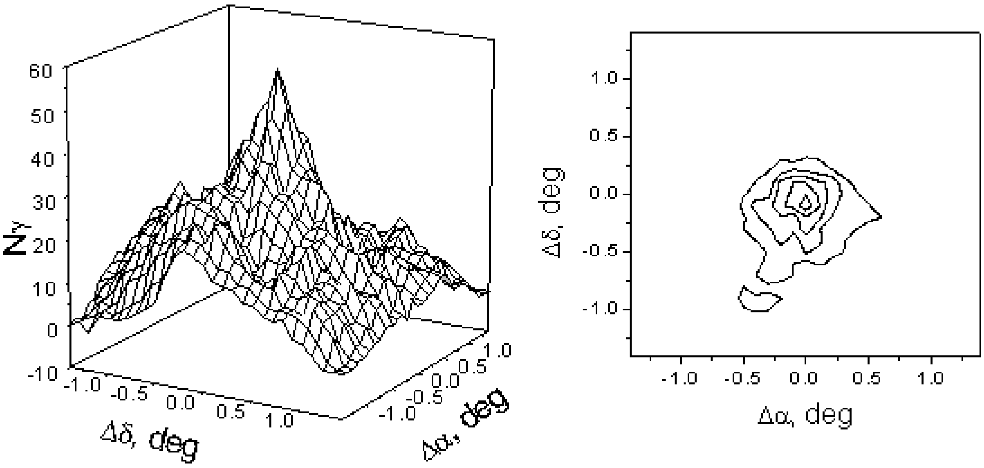

Fig. 2. Left plot: Stereo "map" of the distribution of the γ-ray arrival directions. Right plot: The "map" of isophotes for γ-ray source BL Lac. The highest excess of VHE gamma-quanta appears at (0.0, –0.1). The external isophote corresponds to 29 events. The isophotes step is 6 events

The mean count rate for observing period was equal to (0.116 $\pm$ 0.021) min^{-1}. To convert this count rate to flux we have processed the Crab Nebula observation data gathered in 2002-2004 seasons with a total of 15 hr of source exposure. Was applied the same selection criteria and cuts as for BL Lac. The resulting count rate was equal to (0.109 $\pm$ 0.022) min^{-1}. So the flux from BL Lac expressed as a fraction of the Crab Nebula steady count rate is (1.1 $\pm$ 0.4) Crab.

Using method of trial sources it is possible to find the region of the sky in which a gamma-ray source is located (Akerlof et al., 1991). This method is based on the orientation images of the flashes from gamma-rays in the telescope focal plane toward the source position contrary to the uniform distribution of images of proton showers. Using differences amongst distribution of gamma-like events in the focal plane in ON and OFF modes the position of the true gamma-ray source may be found. In Figures 2 are shown two-dimensional histogram and isophotes of this distribution. The precision of determination of source coordinates by method of trial sources is $\approx 0\overset{\circ}{.}1$.

5 Correlation with X-ray Emission

ASM/RXTE observations of BL Lac object in 2 – 10 keV energy band are summarized in Figure 3. Data for the light curve are quoted as nominal rates in ASM counts per second, where the Crab Nebula flux is about 75 ASM c/s. The mean ASM count rate for epoch, coincident with observations in TeV energy band is (0.308 $\pm$ 0.033) c/s, so that flux from object in 2 – 10 keV energy band equal to (4.1 $\pm$ 0.4)$\cdot 10^{-3}$ of the steady X-ray flux in this energy band from the Crab Nebula.

Once we have the fluxes expressed as a fractions of the Crab Nebula flux in two energy band we may conclude that integral flux from the BL Lac at E> 1 TeV is equal to (286 $\pm$ 124) times the flux in the narrow 2 – 10 keV energy band. So that the ratio of IC and synchrotron luminosities in BL Lac object is high.

Accordingly to Figure 3 object did not expose obviously expressed synchrotron flaring activity in observed period. A slightly enhanced activity was observed in the end of epoch. Two flares, occurred in this period with low statistical significance ($\sim 1\sigma$) and $\approx$10–fold ASM count rate enhancement (MJD52605.6 and 52606.1) were accompanied by a number of less expressed flares (up to 4-fold flux increment) but slightly higher statistical significances. This tendency in flux enhancement from July to December is more evident for average fluxes in darkmoon periods in two energy bands (Figure 4).

The data shown in ASM plot are average for periods which coincide with observations in TeV band or close to them. Both approximating lines have nearly identical slopes that characterize the correlation between data which they are fitting. The correlation coefficient between keV and TeV data sets along with their errors is (0.65 $\pm$ 0.07). Although there occurred synchrotron flare at the beginning of observations, in whole a counting rate rose to the

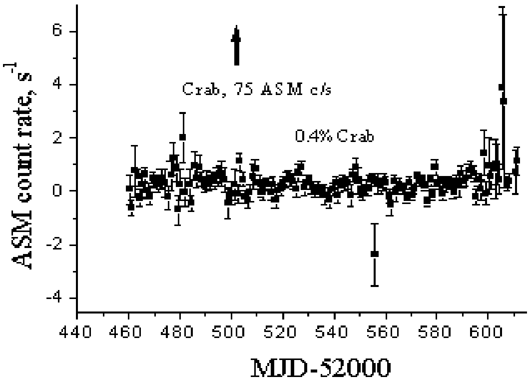

Fig. 3. Time history of the BL Lac emission in 2 – 10 keV energy band (quick-look results provided by the ASM/RXTE team) in the epoch, coincided with the observations in TeV band. Each "one-day average" data point represent the one-day average of the source fluxes from 5 – 10 individual 90 s ASM dwells

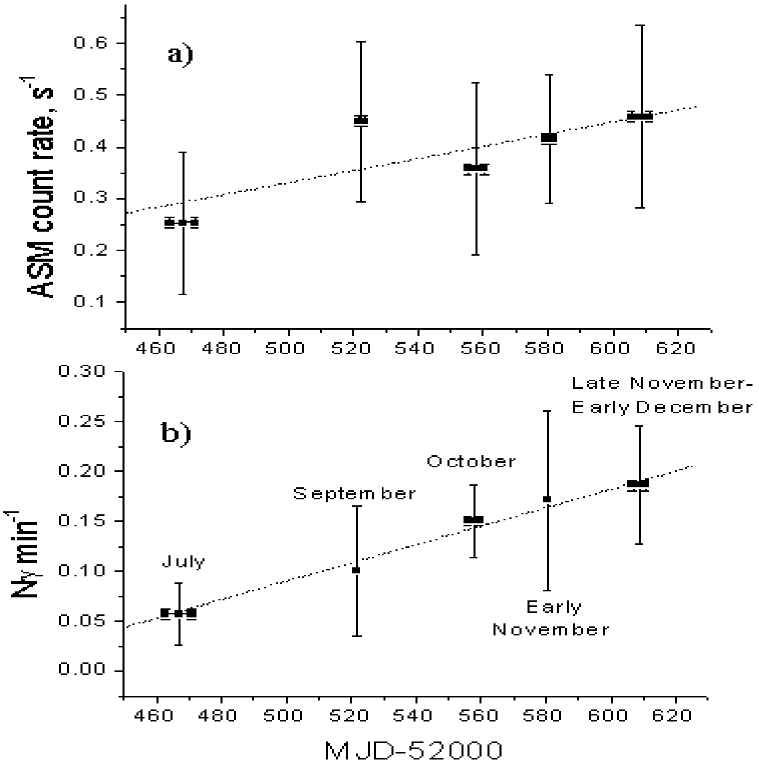

Fig. 4. The comparison of keV (a) and TeV (b) observations of BL Lac. The short dashed lines fit the data along with their errors by least-square method. Error bars are purely statistical

end of observations. So there is an obvious evidence of enhancing activity from quiescent period in July to excited one in November-December.

The averaged flux of TeV γ-rays in the end of observing period was increased by a factor of (3.3 $\pm$ 2.8) relatively to beginning of observations, while the average flux of X-rays was increased by a factor of (1.8 $\pm$ 1.7). The early October flux of VHE photons has the highest statistical confidence (4.2 σ) and differs little from late November/early December data.

6 Conclusion

The detection of VHE γ-rays from BL Lac object is confirmed at the 5.6 σ confidence level. During late November/ early December the source has exhibited enhanced activity in both keV and TeV energy bands. At a whole there is seen a major transition from a rather quiescent state in July to excited state for the rest of observations.

This intensity feature is also evident in the 2 – 10 keV energy band. The correlated variability in both energy bands strongly supports the commonly accepted models in which synchrotron and IC components originate in the same region of the relativistic jet.

References

Aharonian F.A., Akhperjanian A.G. and Barrio J.A. // Astron. Astrophys. 1999. V. 342. P. 69.
Aharonian F., Akhperjanian A., Barrio J. et al. // Astron. Astrophys. 2002. V. 384. L23.
Aharonian F., Akhperjanian A., Beilicke M. et al. // Astron. Astrophys. 2003a. V. 403. L1.
Aharonian F., Akhperjanian A., Beilicke M. et al. // Astron. Astrophys. 2003b. V. 406. L9.
Aharonian F. and Konopelko A.K. // In Kruger National Park Workshop on TeV Gamma Ray Astropohysics, Towards a Major Atmospheric Cerenkov Detector – V. Space Research Unit. WESTPRINT–Potchefstroom. South Africa. Ed. O.C. de Jager. 1997. P. 263.
Akerlof C.W., Cawley M.F., Chantell M. et al. // Astrophys. J. Lett. 1991. V. 377. L. 97.
Bonnet-Bidaud, J.-M. and Chardin, G. // Physics reports. 1998. V. 170. N. 6. P. 326.
Böttcher, M., Marscher, A.P., Ravasio, M. et al. // Astrophys. J. 2003. V. 596. N. 2. P. 847.
Catanese M., Akerlof C. W., Biller S. D. et al. // Astrophys. J. 1997. V. 480. P. 562.
Catanese M., Akerlof C. W., Badran H. M. et al. // Astrophys. J. 1998. V. 501. P. 616.
Costamante L. and Ghisellini G. // Astron. Astrophys. 2002. V. 384. P. 56.
Ghisellini G., Celotti A., Fossati G. et al. // Mon. Not. R. Astron. Soc. 1998. V. 301. P. 451.
Katarzynski K., Sol H. and Kus A. // Astron. Astrophys. 1999. V. 410. P. 101.
Punch M., Akerlof C.W., Cawley M.F. et al. // Nature. 1992. V. 358. P. 477.
Quinn J., Akerlof C.W., Biller S. et al. // Astrophys. J. Lett. 1996. V. 456. L83.
Kalekin O.R. // Izv. Krim. Astrofiz. Observ. 1999. V. 95. P. 173.
Hillas, A.M. // Proc. 19-th Intern. Cosm. Ray Conf. La Jolla. USA. 1985. V. 3. P. 445.
Neshpor Yu.I., Stepanian A.A., Kalekin O.R. et al.// Astron. Lett. 1998. V. 24. N. 3. P. 67.
Neshpor Yu.I., Chalenko N.N., Stepanian A.A. et al. //Astron. Reports. 2001.V. 78. N.4. P. 291
Neshpor Yu.I., Stepanian A.A., Eliseev V.S. et al. // Izv. Krim. Astrofiz. Observ. 2003. V. 99. P. 43.
Neshpor Yu.I., Stepanian A.A., Eliseev V.S. et al. // In Proc. of 28th All-Russian Cosmic Ray Conf. Moscow, June 7–11. 2004. M. MEPHI. P. 109.
Thompson D.J., Bertsch D.L., Dingus B.L. et al. // Astrophys. J. Suppl. Ser. 1995. V. 101. P. 259.
Vladimirsky B.M., Zyskin Yu.L., Kornienko A.P. et al. // Izv. Krim. Astrofiz. Observ. 1994. V. 91. P. 74.